Mineralogical Magazine, December 2013, Vol. 77(8), pp. 3217–3237

The crystal structure of comancheite, $Hg^{2+}_{55}N^{3-}_{24}(OH,NH_2)_4(Cl,Br)_{34}$, and crystal-chemical and spectroscopic discrimination of N^{3-} and O^{2-} anions in Hg^{2+} compounds

M. A. Cooper[1], Y. A. Abdu[1], F. C. Hawthorne[1,]* and A. R. Kampf[2]

[1] Department of Geological Sciences, University of Manitoba, Winnipeg, Manitoba, R3T 2N2, Canada
[2] Mineral Sciences Department, Natural History Museum of Los Angeles County, 900 Exposition Blvd., Los Angeles, California 90007, USA

[*Received 22 June 2013; Accepted 19 November 2013; Associate Editor: A. Christy*]

ABSTRACT

The crystal structure of comancheite, $Hg^{2+}_{55}N^{3-}_{24}(OH,NH_2)_4(Cl,Br)_{34}$, orthorhombic, space group *Pnnm*, a = 18.414(5), b = 21.328(6), c = 6.6976(19) Å, V = 2630(2) Å^3, Z = 1, was solved by direct methods and refined to an R_1 index of 4.3% based on 4160 unique observed reflections. In the structure of comancheite, there are nine crystallographically distinct Hg^{2+} cations, each of which is coordinated by two N^{3-} anions to form near-linear $N^{3-}–Hg^{2+}–N^{3-}$ groups. Four other crystallographically distinct Hg^{2+} cations are coordinated by a mixture of N^{3-}, O^{2-}, $(OH)^-$ and $(NH_2)^-$ anions, and there is a small amount of $[Hg–Hg]^{2+}$ dimer. In addition, there are eight crystallographically distinct halogen sites, three of which are completely occupied by Cl^-, and five of which are occupied by both Cl^- and Br^-. The principal anion, N^{3-}, shows a strong preference for tetrahedral coordination by Hg^{2+}, which results in a strongly bonded three-dimensional $\{–Hg^{2+}–N^{3-}–\}$ framework. This framework is both interrupted and contains large interstices that incorporate additional Hg^{2+} cations, a very small amount of $[Hg^+–Hg^+]^{2+}$ dimer and additional anion species, O^{2-}, $(OH)^-$ and $(NH_2)^-$, that coordinate Hg^{2+}.

Comancheite was described originally as an Hg-oxide mineral. The major change in chemical composition indicated by the present work was approved by the Commission on New Minerals, Nomenclature and Classification of the International Mineralogical Association (Voting Proposal 13-B). The presence of N provides some analytical challenges, particularly in the presence of Hg. New bond-valence parameters were derived for $Hg^{2+}–N^{3-}$ bonds [$R_o(N^{3-})$ = 1.95] using well refined Hg^{2+} structures, and this allows discrimination between $Hg^{2+}–O^{2-}$ and $Hg^{2+}–N^{3-}$ bonds based on the valence-sum rule. Comparison of the Raman spectra of several Hg-bearing minerals shows that peaks in the range 500–700 cm^{-1} are characteristic of $Hg^{2+}–N^{3-}$ stretching vibrations whereas peaks in the range 350–500 cm^{-1} are characteristic of $Hg^{2+}–O^{2-}$ stretching vibrations; $Hg^{2+}–O^{2-}$ and $Hg^{2+}–N^{3-}$ bonds may be discriminated on this basis.

Keywords: comancheite, crystal structure, electron microprobe analysis, infrared spectrum, Raman spectrum, mercury nitride.

Introduction

Comancheite is a secondary mineral from the Mariposa mine, Terlingua district, Brewster County, Texas, USA, described by Roberts *et al.* (1981). It forms tiny orange-red to yellow crystalline masses or stellate crystal groups perched on colourless skeletal calcite, on a matrix of colourless to banded yellow-brown calcite. It was described as a mercury

---

* E-mail: frank_hawthorne@umanitoba.ca
DOI: 10.1180/minmag.2013.077.8.13

oxychloride-bromide mineral with the ideal formula $Hg_{13}(Cl,Br)_8O_9$ (Roberts *et al.*, 1981). The formula was derived assuming that all Hg is present as Hg^{2+}, and that the non-halogen anion is oxygen, leading to the formula $Hg^{2+}_{13}(Cl_{4.5}Br_{3.5})_{\Sigma=8}O_9$ with $Z = 4$. It was noted that the measured refractive indices are noticeably lower than those calculated using the chemical formula and density. As part of a systematic examination of Hg minerals (Cooper and Hawthorne, 2003, 2009; Roberts *et al.*, 2002, 2003*a*,*b*, 2005), we solved the crystal structure of comancheite, and detailed crystal-chemical examination of the results showed that comancheite is not an Hg oxide but an Hg nitride. This prompted further examination on how to distinguish spectroscopically between Hg oxides and Hg nitrides, and the results of both parts of this work are presented here.

Comancheite sample

The crystals of comancheite used in this study were obtained from a micromount specimen in the collections of the Natural History Museum of Los Angeles County, catalogue number 26686. This specimen is part of the Benjamin J. Chromy Collection, bequeathed to the museum in 1985. Mr. Chromy's records indicate that he acquired the original sample in April 1964 from a Lt. Hutchinson. On the micromount specimen, the comancheite occurs on calcite.

Crystal-structure solution and refinement

A crystal of comancheite was attached to a tapered glass fibre and mounted on a Bruker D8 three-circle diffractometer equipped with a rotating-anode generator (Mo$K\alpha$), multilayer optics and an APEX-II detector. A total of 100,805 intensities (29,847 within the Ewald sphere) was collected to 60º2θ using 15 s per 0.3º frames with a crystal-to-detector distance of 5 cm. An empirical absorption correction (SADABS, Sheldrick, 2008) was applied and reflections were corrected for Lorentz, polarization and background effects, averaged and reduced to structure factors. The unit-cell dimensions were obtained by least-squares refinement of 4028 reflections with $I > 10\sigma I$ and are given in Table 1, together with information pertaining to data collection and structure refinement.

All calculations were done with the *SHELXL* PC (Plus) system of programs. Systematic absences in the X-ray diffraction data are consistent with the space group *Pnnm*, and the structure was solved with this symmetry by direct methods and refined with anisotropic-displacement parameters for all atoms. We note that at the completion of refinement, the 50 worst fit reflections output by the program all have $|F_o| > |F_c|$, possibly suggesting a minor overlapping twin component. However, we were unable to refine satisfactorily a model incorporating a merohedral twin component in *Pnnm* or lower-symmetry space groups. Refined atom coordinates and anisotropic-displacement parameters are listed in Table 2, selected interatomic distances are given in Table 3, and refined site-populations of the halogen sites are given in Table 4.

Electron-microprobe analysis

A small crystal of comancheite was immersed in epoxy, polished and carbon-coated. Chemical

TABLE 1. Miscellaneous structural information for comancheite.

a (Å)	18.414(5)	Crystal size (μm)	15 × 20 × 50
b	21.328(6)	Radiation	Mo$K\alpha$
c	6.6976(19)	No. of reflections	100805
V (Å^3)	2630(2)	No. in Ewald sphere	29847
Space group	*Pnnm*	No. unique reflections	4160
Z	1	R_{merge} %	2.4
μ (mm^{-1})	84.1	R_1 %	4.3
D_{calc} (g/cm^3)	8.25	wR_2 %	9.6

Unit formula: $Hg^{2+}_{55}N_{24}(OH,NH_2)_4(Cl_{24.5}Br_{9.5})_{\Sigma=34}$

TABLE 2. Final atom coordinates and displacement parameters (Å^2) for comancheite.

Atom	Occupancy	x	y	z	U^{11}	U^{22}	U^{33}	U^{23}	U^{13}	U^{12}	U_{eq}
Hg(1)		½	½	0	0.0126(4)	0.0193(5)	0.0197(5)	0	0	–0.0024(4)	0.0172(2)
Hg(2)		½	0	0	0.0163(5)	0.0239(6)	0.0203(5)	0	0	0.0041(4)	0.0202(2)
Hg(3)		0.91386(3)	0.11482(3)	0.24975(8)	0.0181(2)	0.0213(3)	0.0147(2)	0.0025(2)	–0.0008(2)	–0.0000(2)	0.01805(11)
Hg(4)		0.50315(4)	0.26909(4)	½	0.0119(3)	0.0299(4)	0.0158(3)	0	0	0.0012(3)	0.01920(16)
Hg(5)		0.65881(3)	0.23803(3)	0.25192(9)	0.0151(2)	0.0380(3)	0.0139(2)	0.0003(2)	0.0024(2)	0.0020(2)	0.02233(13)
Hg(6)		0.81413(4)	0.00970(4)	½	0.0141(3)	0.0250(4)	0.0204(4)	0	0	–0.0040(3)	0.01985(16)
Hg(7)		0.84457(3)	0.45912(3)	0.24695(9)	0.0214(3)	0.0346(3)	0.0148(3)	–0.0021(2)	–0.0039(2)	0.0067(2)	0.02358(13)
Hg(8)		0.74117(4)	0.35931(4)	0	0.0181(4)	0.0230(4)	0.0220(4)	0	0	0.0022(3)	0.02103(17)
Hg(9)		0.81579(4)	0.21879(4)	0	0.0118(3)	0.0227(4)	0.0170(3)	0	0	0.0025(3)	0.01713(15)
Hg(10)		0.93700(5)	0.35021(4)	½	0.0316(4)	0.0226(4)	0.0258(4)	0	0	0.0037(3)	0.02666(19)
Hg(11)	0.62(6)	0.5797(2)	0.1152(5)	½	0.018(2)	0.021(2)	0.0204(16)	0	0	0.0034(8)	0.0200(17)
Hg(12)	0.30(6)	0.5827(8)	0.130(2)	½	0.063(7)	0.041(10)	0.044(4)	0	0	0.002(4)	0.049(4)
Hg(13)	0.846(6)	0.63926(11)	0.43040(10)	0.5231(11)	0.0575(12)	0.0517(11)	0.063(4)	–0.0191(18)	–0.029(2)	–0.0112(9)	0.0575(16)
Hg(14)	0.046(6)	0.4418(16)	0.5324(19)	½	0.037(15)	0.10(3)	0.047(18)	0	0	0.019(15)	0.061(13)
X(1)		0.7123(2)	0.5303(19)	½	0.039(2)	0.054(2)	0.0292(18)	0	0	0.0159(15)	0.0407(12)
X(2)		0.6031(3)	0.1188(2)	0	0.042(3)	0.039(2)	0.052(3)	0	0	–0.0160(18)	0.0446(15)
X(3)		0.7627(2)	0.3392(2)	½	0.036(2)	0.047(3)	0.035(2)	0	0	–0.0168(18)	0.0392(14)
X(4)		0.7642(3)	0.1494(3)	½	0.035(3)	0.055(3)	0.060(3)	0	0	0.027(2)	0.0499(18)
X(5)		0.9695(3)	0.2430(2)	½	0.072(4)	0.025(2)	0.030(3)	0	0	0.006(2)	0.0422(18)
X(6)		0.5858(3)	0.3755(3)	0.2246(10)	0.041(3)	0.058(3)	0.061(4)	–0.017(3)	–0.006(3)	0.012(2)	0.0530(15)
X(7)		0.9148(3)	0.3462(3)	0	0.023(3)	0.027(3)	0.045(4)	0	0	0.006(2)	0.0316(13)
X(8)		½	½	½	0.028(4)	0.026(4)	0.041(5)	0	0	0.008(3)	0.0315(18)
N(1)		0.7180(9)	0.2656(9)	0	0.016(8)	0.024(9)	0.009(7)	0	0	–0.000(7)	0.017(3)
N(2)		0.5949(12)	0.2162(11)	½	0.037(11)	0.038(12)	0.011(8)	0	0	0.012(9)	0.029(4)
N(3)		0.7743(9)	0.4523(10)	0	0.013(7)	0.036(10)	0.008(7)	0	0	0.003(7)	0.019(4)
N(4)		0.9118(10)	0.0578(9)	½	0.020(8)	0.026(9)	0.018(9)	0	0	–0.013(7)	0.022(4)
N(5)		0.9073(9)	0.4463(10)	½	0.009(7)	0.037(11)	0.010(7)	0	0	–0.007(7)	0.019(4)
N(6)		0.9120(8)	0.1701(8)	0	0.008(6)	0.020(8)	0.009(7)	0	0	0.010(6)	0.013(3)
O(7)	0.84(8)	0.5683(13)	0.0232(18)	½							0.028(5)*
O(8)	0.16(8)	0.570(6)	0.048(9)	½							0.028(5)*

* constrained to be equal during refinement.

TABLE 3. Selected interatomic distances (Å) and angles (°) for comancheite.

Hg(1)–N(4)	2.04(2)	×2
N(4)–*Hg*(1)–N(4)	180	
Hg(1)–X(6)	3.437(6)	×4
Hg(1)–X(8)	3.349(1)	×2
Hg(2)–N(5)	2.056(17)	×2
N(5)–*Hg*(2)–N(5)	180(1.0)	
Hg(2)–X(2)	3.166(4)	×2
Hg(3)–N(4)	2.071(12)	
Hg(3)–N(6)	2.046(10)	
N(4)–*Hg*(3)–N(6)	177.8(7)	
Hg(3)–X(1)	3.383(3)	
Hg(3)–X(4)	3.309(4)	
Hg(3)–X(5)	3.366(5)	
Hg(3)–X(6)	3.177(6)	
Hg(3)–X(8)	3.363(1)	
Hg(4)–N(2)	2.03(2)	
Hg(4)–N(6)	2.121(17)	
N(2)–*Hg*(4)–N(6)	176.0(8)	
Hg(4)–X(5)	3.415(2)	×2
Hg(4)–X(6)	3.296(7)	×2
Hg(4)–X(7)	2.949(6)	
Hg(5)–N(1)	2.093(10)	
Hg(5)–N(2)	2.088(14)	
N(1)–*Hg*(5)–N(2)	175.8(8)	
Hg(5)–X(2)	3.220(4)	
Hg(5)–X(3)	3.328(4)	
Hg(5)–X(4)	3.178(4)	
Hg(5)–X(5)	3.894(6)	
Hg(5)–X(6)	3.230(6)	
Hg(6)–N(3)	2.037(18)	
Hg(6)–N(4)	2.071(17)	
N(3)–*Hg*(6)–N(4)	172.8(8)	
Hg(6)–X(1)	3.413(1)	×2
Hg(6)–X(4)	3.118(5)	
Hg(6)–X(6)	3.723(7)	×2
Hg(7)–N(3)	2.105(11)	
Hg(7)–N(5)	2.069(10)	
N(3)–*Hg*(7)–N(5)	167.9(8)	
Hg(7)–X(1)	3.333(3)	
Hg(7)–X(2)	3.924(5)	
Hg(7)–X(3)	3.419(4)	
Hg(7)–X(7)	3.195(5)	
Hg(8)–N(1)	2.043(18)	
Hg(8)–N(3)	2.08(2)	
N(1)–*Hg*(8)–N(3)	175.0(7)	
Hg(8)–X(3)	3.400(1)	×2
Hg(8)–X(6)	3.251(6)	×2
Hg(8)–X(7)	3.209(6)	
Hg(9)–N(1)	2.060(18)	
Hg(9)–N(6)	2.054(15)	
N(1)–*Hg*(9)–N(6)	178.6(7)	
Hg(9)–X(4)	3.783(3)	×2
Hg(9)–X(7)	3.272(7)	
Hg(10)–N(5)	2.12(2)	
Hg(10)–X(5)	2.364(5)	
N(5)–*Hg*(10)–X(5)	179.7(5)	
Hg(10)–X(2)	3.130(5)	
Hg(10)–X(3)	3.218(5)	
Hg(10)–X(7)	3.375(1)	×2
Hg(11)–N(2)	2.17(3)	
Hg(11)–O(7)	1.97(4)	
N(2)–*Hg*(11)–N(7)	179.8(1.2)	
Hg(11)–X(2)	3.377(1)	×2
Hg(11)–X(4)	3.474(7)	
Hg(11)–X(7)	3.148(7)	
Hg(12)–N(2)	1.86(5)	
Hg(12)–O(8)	1.75(19)	
N(2)–*Hg*(12)–N(7)	179(4)	
Hg(12)–X(2)	3.378(3)	×2
Hg(12)–X(4)	3.37(2)	
Hg(12)–X(7)	3.136(14)	
Hg(13)–X(1)	2.525(5)	
Hg(13)–X(3)	2.996(6)	
Hg(13)–X(6)	2.280(8)	
Hg(13)–X(6)	2.518(8)	
Hg(13)–X(8)	2.967(2)	
Hg(14)–*Hg*(14)	2.55(6)	
Hg(14)–X(1)	3.14(4)	
Hg(14)–X(6)	2.74(3)	×2
O(7)–O(8)	0.54(16)	
Hg(11)–*Hg*(12)	0.31(4)	
Hg(13)–*Hg*(13)	0.310(14)	
Hg(13)–*Hg*(14)	1.70(3)	
Hg(14)–X(8)	1.28(3)	

analysis was done using a Cameca SX-100 electron microprobe operating in wavelength-dispersion mode at an accelerating voltage of 15 kV and a specimen current of 5 nA. We used the largest beam we could (5 µm) given the small crystal size. A test point showed that X-ray counts for the major elements (Hg, Cl, Br) were reasonably stable over the analysis time, although

TABLE 4. Refined site-populations (a.p.f.u.) for the halogen sites in comancheite.

Site	Cl	Br
X(1)	1.11	2.89
X(2)	2.02	1.98
X(3)	2.23	1.77
X(4)	2.36	1.64
X(5)	2.76	1.24
X(6)	8	–
X(7)	4	–
X(8)	2	–
Sum	24.48	9.52

visible sample burning was evident at the end of the analysis. An attempt to measure the N content was unsuccessful, presumably due to the extreme absorption effects of the Hg present in the crystal. The following standards were used: Hg, cinnabar; Cl, tugtupite; Br, AgBr. Two point determinations were averaged and are presented in Table 5.

Raman and FTIR spectroscopy

Raman spectra in the range 100–1200 cm^{-1} were collected in back-scattered mode using a HORIBA Jobin Yvon-LabRAM ARAMIS integrated confocal micro-Raman system equipped with a 460 mm focal-length spectrograph and a multichannel air-cooled (–70ºC) CCD detector. A magnification of 100 × was used with an estimated spot size of ~1 µm, a 1800 gr/mm grating, and a 785 nm excitation laser. The wavenumber was calibrated using the 520.7 cm^{-1} line of elemental Si. Transmission FTIR spectra were collected on a single crystal using a Bruker Hyperion 2000 IR microscope equipped with a liquid-nitrogen-cooled MCT detector. Spectra over the range 4000–650 cm^{-1} were obtained by averaging 100 scans with a resolution of 4 cm^{-1}.

Crystal structure

Here, we will focus on the structure of comancheite and the issue of identifying the presence of nitrogen in the structures of Hg-minerals. We are currently working on several other Hg-nitride minerals and will compare their crystal chemistry with that of other known structures (e.g. Borisov *et al.*, 2005) in due course.

N sites

The Hg and halogen part of the structure ($Hg^{2+}_{55}X_{34}$, X = Cl,Br) carries a net charge of 76^{+} that must be compensated by the remaining 28 anions of lower scattering power. If these remaining anions were all O^{2-}, as indicated by the original formula of Roberts *et al.* (1981), there would be insufficient negative charge for electroneutrality (i.e. 56^{-}). Thus anions with negative charge greater than 2^{-} must occupy all (or nearly all) of the remaining anion sites, and we have assigned N^{3-} to the

TABLE 5. Chemical composition and unit-cell content for comancheite.

	Roberts *et al.* (1981)			This study			
	EMPA (wt.%)	Atoms*		SREF (wt.%)**	Atoms		EMPA (wt.%)
Hg	83.1	55.0		84.45	55.0		86.3
Cl	5.1	19.1	33.9	6.65	24.5	34.0	6.1
Br	8.9	14.8		5.81	9.5		6.1
Total	97.1			96.91			98.5
N				2.57	24		
O				0.49	4		
H				0.03	4		
Total				100			

* normalized to 55 Hg atoms;

** using the formula $Hg_{55}(Cl_{24.5}Br_{9.5})_{\Sigma=34}N_{24}(OH)_4$.

majority of these sites. There are 8 sites (giving 28 a.p.f.u.) of lower scattering power that are dominantly N atoms. These sites have to provide a charge of 76^-, and the limiting values for these charges are $20 \times 3^- + 8 \times 2^- = 76^-$ and $24 \times 3^- + 4 \times 1^- = 76^-$ for non-trivalent anions that are all divalent and all univalent, respectively. As we were unable to determine N chemically, we approached the task of N identification using crystal-chemical arguments (anion coordination, bond valence) and both Raman and infrared spectroscopy (see below).

Hg sites

The *Hg*(1–9) sites are all fully occupied by Hg^{2+}, are coordinated by two adjacent N^{3-} anions (Hg^{2+}–N^{3-} range = 2.03–2.12 Å), and form approximately linear N^{3-}–Hg^{2+}–N^{3-} groups; the range in (N^{3-}–Hg^{2+}–N^{3-}) angle = 167.9–180º (Fig. 1, Table 3). The *Hg*(10) site is coordinated by a neighbouring N^{3-} anion on one side (Hg^{2+}–N^{3-} = 2.12 Å), and a halogen on the opposite side (Hg^{2+}–X = 2.364 Å), with a near linear (N^{3-}–Hg^{2+}-X) angle of 179.7º. The *Hg*(11) and *Hg*(12) sites are occupied by Hg^{2+} and are separated by only 0.31 Å, and hence cannot both be locally occupied. The *Hg*(11) occupancy refined to 0.62(6) and the *Hg*(12) occupancy to 0.30(6) to give an aggregate occupancy of 0.92(6); the implied vacancy occupancy is 0.08(6). We may evaluate the significance of this value by testing if it is different from zero at the 99% confidence limit. The value divided by its standard deviation is 0.08/0.06 = 1.33, significantly less than the value of 2.58 at the 99% confidence limit, and hence we cannot reject the hypothesis that the value is equal to zero. To either side of the *Hg*(11)–*Hg*(12) pair are N^{3-} and O^{2-} anions from 1.86 to 2.17 Å away from the Hg^{2+} atoms, with [N^{3-}–Hg^{2+}–$(OH)^-$, $(NH_2)^-$] angles of 180 and 179º [the O(7) and O(8) sites are occupied by $(OH)^-$ or $(NH_2)^-$ groups]. The *Hg*(1–12) sites are coordinated additionally by distant halogens (Hg^{2+}–X > 3 Å) [X = Cl, Br] located at a large angle to the near-linear (N^{3-},X)–Hg^{2+}-(N^{3-},O^{2-}) axis (Fig. 1). The coordination environments for *Hg*(1–12) are typical for Hg^{2+}, although Hg^{2+}–(N^{3-},O^{2-}) distances less than 2 Å observed for the disordered *Hg*(11)–*Hg*(12) pair are shorter than normal. The *Hg*(11)–*Hg*(12) part of the structure is a termination of the {–Hg^{2+}–N^{3-}–} net and is characterized by positional disorder and larger atom-displacements; the interatomic distances within this disordered region are less precise than those in the ordered {–Hg^{2+}–N^{3-}–} net. The *Hg*(13) site refined to a position slightly off the mirror plane (*m* at *z* = ½), and is disordered across the mirror with an *Hg*(13)–*Hg*(13)′ separation of 0.31 Å (Fig. 1). The refined occupancy for the *Hg*(13) site is 0.846(6), significantly less than full occupancy. The *Hg*(13) site is not close to any N^{3-} anions, and occurs within an expanded void region of the {–Hg^{2+}–N^{3-}–} net, forming five close contacts to halogen atoms (Hg^{2+}–X range = 2.28–3.00 Å). Although this is a less typical coordination for Hg^{2+}, the bond valence incident at the *Hg*(13) site indicates clearly that the site is occupied by Hg^{2+}. Near the end of structure refinement, a minor peak observed in the difference-Fourier map close to the *Hg*(13) site (i.e. *Hg*(13)-peak = 1.70 Å) was included in the refinement as a possible additional *Hg* site [*Hg*(14)] (Figs 1,2).

The refined occupancy for *Hg*(14) is 0.046(6); is this significantly different from zero? The value divided by its standard deviation is 0.046/0.006 = 7.67, significantly greater than the value of 2.58 at the 99% confidence limit, and hence we can reject the hypothesis that this value is equal to zero. The *Hg*(14) site is 2.55(6) Å from another *Hg*(14) site. This ~2.5 Å separation is in close agreement with the Hg^{1+}–Hg^{1+} distances observed in Hg compounds containing $[Hg–Hg]^{2+}$ dimers (e.g. Cooper and Hawthorne, 2009 and references therein). Although the overall Hg contribution by the *Hg*(14) site is marginal, we have included it as a minor $[Hg–Hg]^{2+}$ occurrence within the {–Hg^{2+}–N^{3-}–} net of comancheite. Note that the halogen at X(8) would be absent where the $[Hg–Hg]^{2+}$ dimer is present locally. The Hg^{2+} content summed over the *Hg*(1)–*Hg*(13) sites gives 55.1 Hg^{2+} atoms p.f.u.

Halogen sites

There are five halogen sites, *X*(1)–*X*(5), that have refined site-scattering values (Hawthorne *et al.*, 1995) lying between Cl and Br. We assigned both Cl and Br scattering factors to each site under the constraint of full occupancy. The *X*(6)–*X*(8) sites each refined to full occupancy by Cl, and were fixed as such in the final refinement cycle. The combined site-occupancies over the eight halogen sites give a total of 24.5 Cl atoms and 9.5 Br atoms (Table 4).

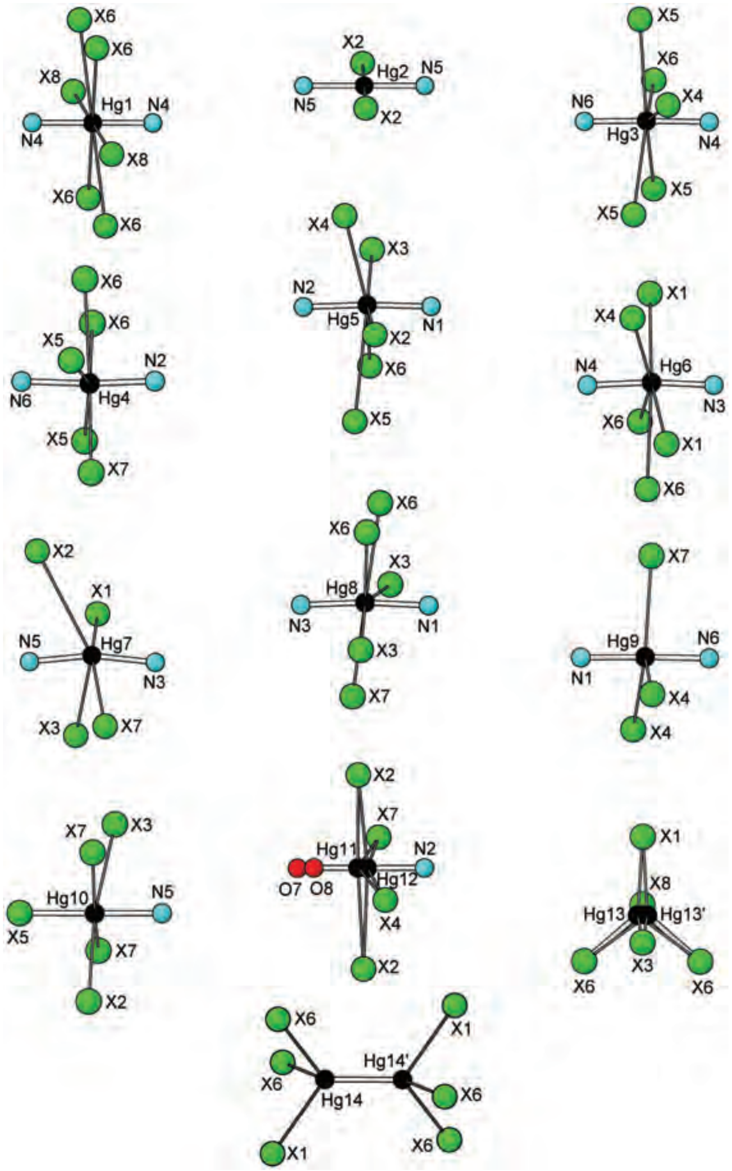

FIG. 1. Coordination of the Hg atoms in comancheite. Hg atoms: black circles, N atoms: blue circles, halogen atoms: green circles, (OH/NH_2) groups: red circles; thick lines: strong axial bonds, thin lines: weaker meridional bonds.

Hg and halogen content of structure

Structure refinement gives 55.1 Hg^{2+} and 34 halide (24.5 Cl^- + 9.5 Br^-) ions in the unit cell. The original electron-microprobe data of Roberts *et al*. (1981), when normalized to 55 Hg atoms, gives a total of 33.9 halogen atoms, in almost exact agreement with the structure results (Table 5). Both our electron-microprobe analysis (Table 5) and the occupancies derived from structure refinement (Table 4) suggest that the two comancheite crystals examined in the present study (electron-microprobe crystal and structure crystal) are slightly more enriched in Cl relative to Br, compared with the comancheite examined by Roberts *et al.* (1981).

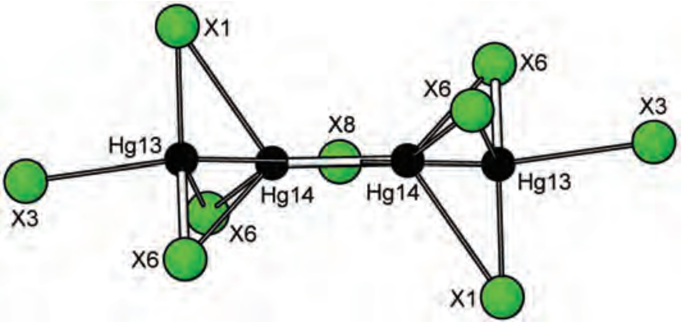

FIG. 2. The overlapping halogen-coordinated environments of the Hg(13) and Hg(14) atoms in comancheite; legend as in Fig. 1.

Bond-valence discrimination of O^{2-} and N^{3-} in Hg^{2+} compounds

Using the available structural data from the ICSD (Inorganic Crystal Structure Database) for Hg^{2+} compounds of oxygen and nitrogen, we selected six well refined structures that are well ordered and contain one or more anions (O^{2-} or N^{3-}) that are coordinated only by Hg^{2+} (Table 6). For the structures containing one or more O^{2-} anions coordinated only by Hg^{2+}, the coordination of O^{2-} varies from [3] to [4]. Where O^{2-} is coordinated by three Hg^{2+} cations, the <O–Hg> distance is ~2.07 Å. Where O^{2-} is coordinated by four Hg^{2+} atoms, there are two short O–Hg^{2+} distances of ~2.06 Å, an intermediate O–Hg^{2+} distance of ~2.2 Å and a longer O–Hg^{2+} distance between ~2.5 and 3.0 Å. Where the bond-valence curve for Hg^{2+}–O^{2-} is used (R_o = 1.93, Brese and O'Keeffe, 1991), the bond-valence sums at the O^{2-} anions range from 1.99 to 2.10 vu. Our search of the ICSD for Hg^{2+}–N^{3-} compounds in which the N^{3-} anion is bonded only to Hg^{2+} gave just two structures: kleinite and synthetic $(Hg_2N)(NO_3)$. In these two structures, there are four independent N^{3-} atoms, each of which is coordinated by four Hg^{2+} atoms (Table 6). The four <N–Hg> distances range from 2.050 to 2.072 Å, and there is little variation between individual N^{3-}–Hg^{2+} distances. We found only one published value for an Hg^{2+}–N^{3-} bond-valence relation: R_o = 2.02 (Brese and O'Keeffe, 1991). Using this relation, the calculated bond-valence sums at the N^{3-} anions range from 3.47 to 3.70 vu, indicating a problem with the bond-valence parameters. The range of data for these structures is rather limited, and with this in mind, we retained the *b* value of 0.37 and considered variations in R_o (the current R_o value is 2.02). Using the observed Hg^{2+}–N^{3-} distances in kleinite and synthetic $(Hg_2N)(NO_3)$, we derived an R_o value of 1.95 which results in reasonable bond-valence sums at the N^{3-} anions (i.e. 2.87–3.05 vu). The 2.87 vu sum is for the single N^{3-}–Hg^{2+} environment in kleinite, which seems a slightly poorer-quality refinement (i.e. *R* = 7.4%) than that of $(Hg_2N)(NO_3)$. The three N^{3-}–Hg^{2+} environments in the better refined (i.e. *R* = 3.9%) $(Hg_2N)(NO_3)$ structure give bond-valence sums at the N^{3-} anions from 2.98 to 3.05 vu using the R_o value of 1.95. Although there is a significant difference between the formal charges of O^{2-} and N^{3-}, the difference between the R_o values used for each, i.e. $R_o(O^{2-})$ = 1.93; $R_o(N^{3-})$ = 1.95, is marginal. The differences in incident bond-valence at the anions (O^{2-} *vs.* N^{3-}) are due mainly to coordination differences: the N^{3-} anion is typically coordinated by four Hg^{2+} cations, and the O^{2-} anion is typically coordinated by no more than three Hg^{2+} cations. The anion bond-valence sums in Table 6 denoted in bold separate the Hg^{2+}-compounds into two distinct anion groups (N^{3-} *vs.* O^{2-}), and suggest that the values $R_o(Hg^{2+}–O^{2-})$ = 1.93 and $R_o(Hg^{2+}–N^{3-})$ = 1.95 can identify reliably the anion coordinated by Hg^{2+} in a structure. In comancheite, the N(1–6) anion environments are presented in Fig. 3; each anion is tetrahedrally coordinated by Hg^{2+} cations and has an incident bond-valence sum near the ideal value of 3 vu [calculated using $R_o(Hg^{2+}–N^{3-})$ = 1.95]. We conclude that the N(1–6) anion sites in comancheite are occupied by N^{3-}.

Other anions in comancheite

In comancheite, one of the low-scattering-power anions [O(7),O(8)] is coordinated by only one

TABLE 6. Coordination environments and bond valences for N^{3-} and O^{2-}-bearing Hg^{2+} compounds from ICSD.

Compound	Ref.	Y_{anion}	$Y{-}Hg^{2+}$ (Å)	$O^{2-}_{Ro=1.93}$	$N^{3-}_{Ro=2.02}$	$N^{3-}_{Ro=1.95}$
Kleinite	[1]	N^{3-}	2.071	0.68	0.87	0.72
$(Hg_2N)((SO_4)_{0.25}Cl_{0.5})(H_2O)_{0.5}$			2.071	0.68	0.87	0.72
			2.071	0.68	0.87	0.72
			2.075	0.68	0.86	0.71
				2.72	3.47	**2.87**
$(Hg_2N)(NO_3)$	[2]	N^{3-}	2.040	0.74	0.95	0.78
			2.040	0.74	0.95	0.78
			2.075	0.68	0.86	0.71
			2.075	0.68	0.86	0.71
				2.84	3.62	**2.98**
		N^{3-}	2.041	0.74	0.94	0.78
			2.043	0.74	0.94	0.78
			2.053	0.72	0.91	0.76
			2.067	0.69	0.88	0.73
				2.89	3.67	**3.05**
		N^{3-}	2.035	0.75	0.96	0.79
			2.037	0.75	0.96	0.79
			2.046	0.73	0.93	0.77
			2.081	0.85	0.66	0.70
				2.89	3.70	**3.05**
$K_2[O(HgSO_3)_3]$	[3]	O^{2-}	2.049	0.72	0.92	0.77
			2.084	0.66	0.84	0.70
			2.084	0.66	0.84	0.70
				2.04	2.60	2.17
$Hg(SeO_4)(HgO)$	[4]	O^{2-}	2.033	0.76	0.97	0.80
			2.061	0.70	0.90	0.74
			2.163	0.53	0.68	0.56
			2.952	0.06	0.08	0.07
				2.05	2.63	2.17
		O^{2-}	2.047	0.73	0.93	0.77
			2.050	0.72	0.92	0.76
			2.089	0.65	0.83	0.69
				2.10	2.68	2.22
$(HgSeO_3)(HgO)(H_2O)_{0.167}$	[5]	O^{2-}	2.073	0.68	0.87	0.72
			2.075	0.68	0.86	0.71
			2.243	0.43	0.55	0.45
			2.442	0.25	0.32	0.26
				2.04	2.60	2.14
Pinchite	[6]	O^{2-}	2.045	0.73	0.93	0.77
$Hg_5Cl_2O_4$			2.057	0.71	0.90	0.75
			2.245	0.43	0.54	0.45
			2.707	0.12	0.16	0.13
				1.99	2.53	2.10

References: [1] Giester *et al.* (1996); [2] Nockemann and Meyer (2002); [3] Weil *et al.* (2008); [4] Weil (2002*a*); [5] Weil (2002*b*); [6] Hawthorne *et al.* (1994).

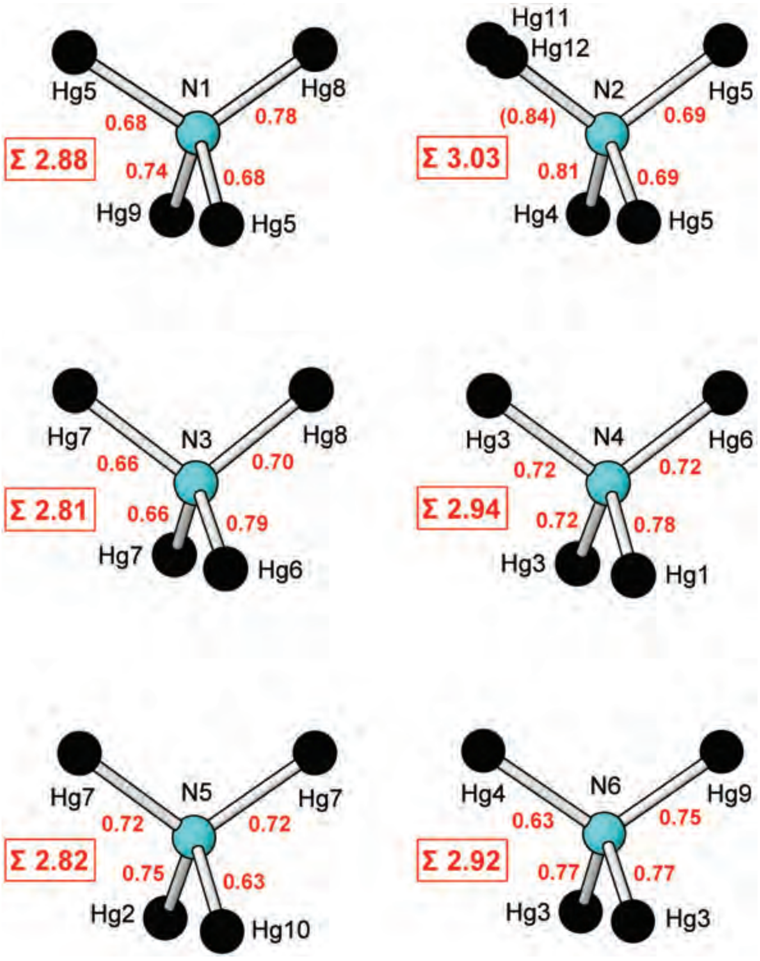

FIG. 3. The tetrahedral coordination environments of the N(1–6) atoms in comancheite; legend as in Fig. 1, red values: bond valences using $R_o[Hg^{2+}–N^{3-}] = 1.95$.

Hg^{2+} cation [Hg(11),Hg(12)], and there must be one or more H atoms also associated with this anion. Potential H-bearing candidates for this anion could be $YH_n = (NH_3)^0$, $(NH_2)^-$, $(NH)^{2-}$, $(OH)^-$ or $(H_2O)^0$. To better understand the $Hg^{2+}–YH_n$ bond-valence variation as a function of YH_n identity, we have compiled structural data from the ICSD in which the protonated anion Y (N^{3-} or O^{2-}) bonds to Hg^{2+} only (Tables 7, 8). All of the $Hg^{2+}_m–NH_n$ environments contain N^{3-} in [4]-coordination (i.e. $m + n = 4$) , whereas the Hg^{2+}_m-OH_n environments generally contain the O^{2-} anion in [3]-coordination (i.e. $m + n = 3$) (Tables 7, 8). In a few instances, the O^{2-} anion is [4]-coordinated by H and Hg^{2+} atoms, but in these cases, one or more of the $Hg^{2+}–O$ distances is notably longer. The range in incident bond-valence at the respective Y anions (from all $Hg^{2+}–Y$ contacts in Tables 6, 7 and 8) is presented in Fig. 4, calculated using the bond-valence parameters $R_o(Hg^{2+}–O^{2-}) = 1.93$ and $R_o(Hg^{2+}–N^{3-}) = 1.95$. The vertical dashed lines separate the fields of incident bond-valence sums at the Y anion for Y = N^{3-} and O^{2-} in relation to the formal charge of the respective YH_n species. In comancheite, the O(7) and O(8) sites are separated by only 0.5 Å and represent a terminal anion (N^{3-} or O^{2-}) attached to the Hg(11)–Hg(12) cation. The occupancies of the *Hg*(11) and O(7) sites are high, and the

TABLE 7. Coordination environments and bond valences for NH_n-bearing Hg^{2+} compounds from ICSD.

Compound	Ref.	NH_n	NH_n–Hg^{2+} (Å)	$N^{3-}_{Ro=1.95}$
$(Hg(NH_3)_4)(ClO_4)_2$ (monoclinic)	[1]	$(NH_3)^0$ $(NH_3)^0$ $(NH_3)^0$ $(NH_3)^0$	2.247 2.286 2.241 2.286	0.45 0.40 0.46 0.40
$(Hg(NH_3)_4)(ClO_4)_2$ (orthorhombic)	[2]	$(NH_3)^0$ $(NH_3)^0$ $(NH_3)^0$	2.277 2.255 2.175	0.41 0.44 0.54
$(Hg(NH_3)_2)(HgCl_3)_2$	[1]	$(NH_3)^0$	2.074	0.72
$(Hg(NH_3))(SeO_3)$	[3]	$(NH_3)^0$	2.100	0.67
$(Hg(NH_3)_2I_2)_2S_4N_4$	[4]	$(NH_3)^0$	2.297	0.39
$HgCl(NH_2)$	[5]	$(NH_2)^{1-}$	2.075 2.075	0.71 0.71 1.42
$(NH_4)(Hg_3(NH)_2)(NO_3)_3$	[6]	$(NH)^{2-}$	2.071 2.071 2.071	0.72 0.72 0.72 2.16

References: [1] Nockemann and Meyer (2003); [2] Nilsson *et al.* (2008); [3] Koskenlinna *et al.* (1996); [4] Martan and Weiss (1984); [5] Leineweber and Jacobs (2000); [6] Nockemann and Meyer (2002).

Hg(11)–O(7) separation is 1.97(4) Å. The bond-valence parameters for Hg^{2+}–O^{2-} and Hg^{2+}–N^{3-} gives 0.90 and 0.95 vu, respectively, for this bond length, which is midway between the fields for neutral (NH_3, H_2O) and univalent (NH_2^-, OH^-) anions. The lesser-occupied *Hg*(12) and O(8) sites [Hg(12)–O(8) = 1.75(19) Å] suggest a greater relative bond-valence value for this pair of

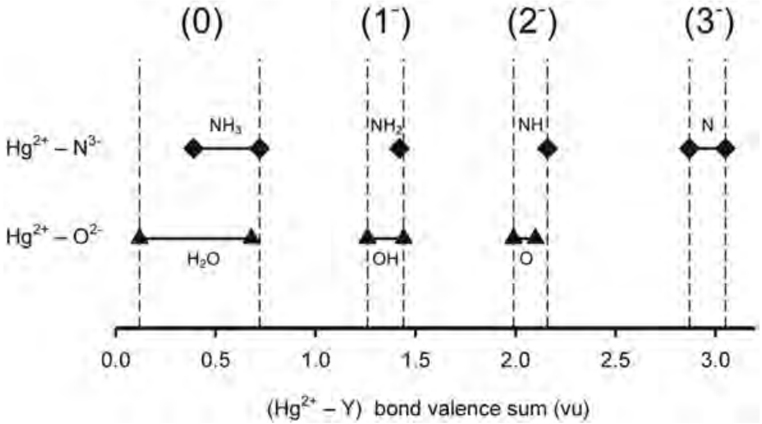

FIG. 4. Bond-valence summations at the N^{3-} and O^{2-} anions in Hg^{2+} compounds resulting from the Hg^{2+}-anion contributions alone; data plotted from Tables 6–8; vertical dashed lines mark experimental bond-valence sums at the Y-anion in relation to the formal charge of the (YH_n) species.

TABLE 8. Coordination environments and bond valences for OH_n-bearing Hg^{2+} compounds from ICSD.

Compound	Ref.	OH_n	OH_n–Hg^{2+} (Å)	$O^{2-}_{Ro=1.93}$
$Hg_2(OH)_2SiF_6(H_2O)_2$	[1]	$(H_2O)^0$	2.549	0.19
$Hg_2(P_2O_7)(H_2O)_2$	[2]	$(H_2O)^0$	2.708	0.12
		$(H_2O)^0$	2.527	0.20
			2.639	0.15
				0.35
$Hg_3(OH)_2(SO_4)_2(H_2O)$	[3]	$(H_2O)^0$	2.659	0.14
			2.659	0.14
				0.28
$HgFeF_5(H_2O)_2$	[4]	$(H_2O)^0$	2.107	0.62
$HgF_2(H_2O)_2$	[5]	$(H_2O)^0$	2.385	0.29
			2.405	0.28
				0.57
$Hg(BrO_3)_2(H_2O)_2$	[6]	$(H_2O)^0$	2.341	0.33
$Hg_2(SeO_3)_2(H_2O)$	[7]	$(H_2O)^0$	2.072	0.68
$Hg(SeO_4)(H_2O)$	[8]	$(H_2O)^0$	2.382	0.29
			2.499	0.21
				0.50
$Hg(SO_4)(H_2O)$	[9]	$(H_2O)^0$	2.228	0.45
$Hg(CrO_4)(H_2O)$	[10]	$(H_2O)^0$	2.300	0.37
$(Hg(H_2O)_6)(ClO_4)_2$	[11]	$(H_2O)^0$	2.342	0.33
$(Hg(H_2O)_2)(CF_3)_2(SO_3)_2$	[12]	$(H_2O)^0$	2.113	0.61
		$(H_2O)^0$	2.114	0.61
$(Hg(OH))(NO_3)(H_2O)$	[13]	$(H_2O)^0$	2.660	0.14
			2.562	0.18
				0.32
$Hg_2(OH)_2SiF_6(H_2O)_2$	[1]	$(OH)^-$	2.035	0.75
			2.119	0.60
				1.35
$Hg_3(OH)_2(SO_4)_2(H_2O)$	[3]	$(OH)^-$	2.058	0.71
			2.149	0.55
				1.26
$Hg_2FeF_5(OH)_2(H_2O)$	[14]	$(OH)^-$	2.064	0.70
			2.064	0.70
				1.40
$Hg_2(NO_3)_2)(Hg(OH)(NO_3))(Hg(NO_3)_2)(HgO)_4$	[15]	$(OH)^-$	2.066	0.69
			2.066	0.69
				1.38
$Hg(OH)(BrO_3)$	[16]	$(OH)^-$	2.066	0.69
			2.066	0.69
				1.38

Table 8 (*contd.*)

Compound	Ref.	OH_n	OH_n–Hg^{2+} (Å)	$O^{2-}_{Ro=1.93}$
$Hg(OH)(ClO_3)$	[17]	$(OH)^-$	2.051	0.72
			2.051	0.72
				1.44
$HgF(OH)$	[18]	$(OH)^-$	2.097	0.64
			2.119	0.60
			2.694	0.13
				1.37

References: [1] Golovastikov (1984); [2] Weil (2003); [3] Aurivillius and Stålhandske (1976); [4] Fourquet *et al.* (1985); [5] Bukvetskii *et al.* (1976); [6] Aurivillius and Stålhandske (1981); [7] Koskenlinna and Valkonen (1996); [8] Stålhandske (1978); [9] Stålhandske (1980); [10] Stöger and Weil (2006); [11] Johansson and Sandström (1978); [12] Molla-Abbassi *et al.* (2002); [13] Nolte *et al.* (2006); [14] Courant *et al.* (1985); [15] Weil (2005); [16] Björnlund (1971); [17] Göbbels and Wickleder (2004); [18] Stålhandske (1979).

ions. We are unable to make a conclusive identification of the aggregate O(7),O(8) anion from a bond-valence perspective alone. The O(7),O(8) anions contribute 4 a.p.f.u., and simple electroneutrality arguments suggest that this anion is dominantly univalent, i.e. $(OH)^-$ or $(NH_2)^-$.

Spectroscopic discrimination of O^{2-} and N^{3-} in Hg^{2+} compounds

The Raman spectrum of comancheite is shown in Fig. 5. The stretching vibrations of Hg^{2+}–O^{2-} occur usually at ~425 cm^{-1} (Sandström, 1978) and those of Hg^{2+}–N^{3-} are observed at ~560 cm^{-1} (Morzyk *et al.*, 1999). In Fig. 6, we compare the Raman spectrum of comancheite, in the range 350–750 cm^{-1}, with the spectra of some Hg-containing minerals (wattersite, edgarbaileyite, mosesite, kleinite and terlinguacreekite) obtained from the RRUFF Raman database. The dashed line in Fig. 6 separates the Raman peaks due to the Hg^{2+}–O^{2-} stretching vibrations (350–500 cm^{-1}) from those of the Hg^{2+}–N^{3-} stretching vibrations (500–700 cm^{-1}). The Raman peaks of comancheite recorded in the

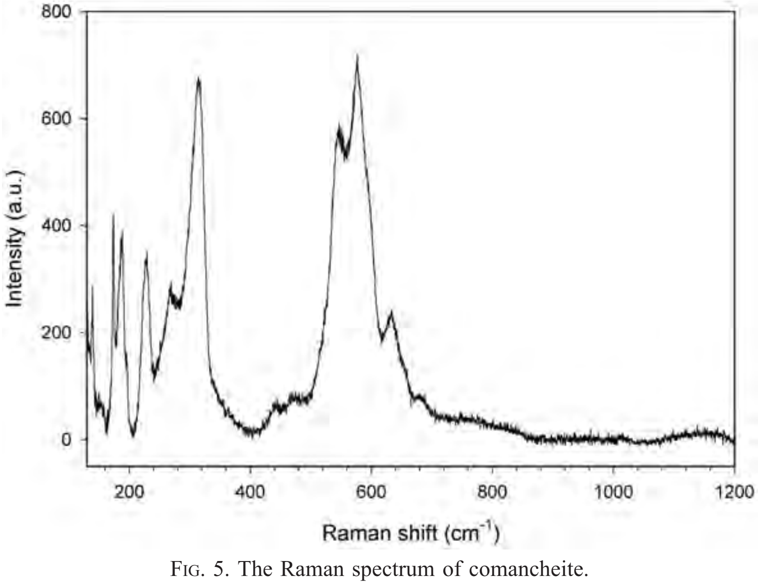

FIG. 5. The Raman spectrum of comancheite.

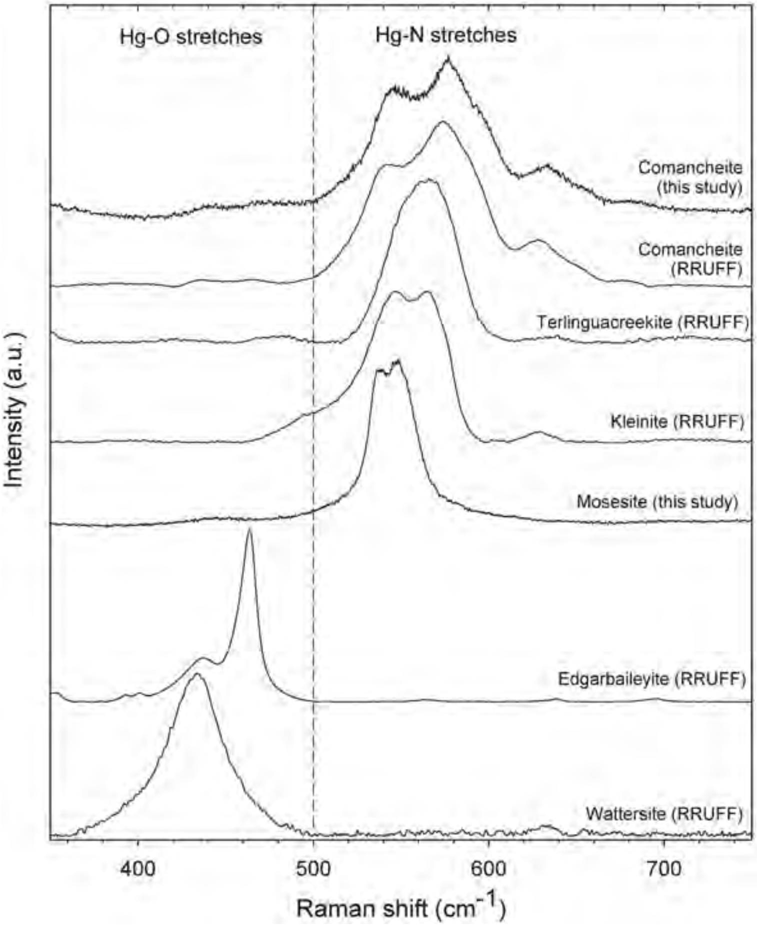

FIG. 6. Raman spectra in the range (350–750 cm^{-1}) of some Hg-containing minerals, separating Hg^{2+}-O^{2-} and Hg^{2+}–N^{3-} stretching peaks.

present work are identical to those of comancheite from the RRUFF database, and they fall in the Hg^{2+}–N^{3-} stretching region. This indicates that N^{3-} is the major anion bonded to Hg^{2+} in comancheite. Thus in the Raman spectrum of comancheite (Fig. 5), we assign the prominent peaks at 545 and 577 cm^{-1}, along with the shoulder at 633 cm^{-1}, to Hg^{2+}–N^{3-} stretching vibrations. The low-intensity bands centred at 470 and 440 cm^{-1} may be assigned to the Hg^{2+}–$(OH)^{-}$ stretching vibrations, in accord with the presence of a small number of $(OH)^{-}$ groups in the structure, which is confirmed by FTIR (see below). The peak at 315 cm^{-1} and the shoulder at 268 cm^{-1} may be assigned to the Hg^{2+}–Cl^{-} and Hg^{2+}–Br^{-} stretching vibrations, respectively, and the two peaks at 228 and 188 cm^{-1} to the Hg^{2+}–N^{3-}–Hg^{2+} bending vibrations. The sharp peak at 174 cm^{-1} is assigned to Hg^{+}–Hg^{+} stretching vibrations.

The FTIR spectrum of comancheite, in the range 3800–1400 cm^{-1}, is shown in Fig. 7. The strong peak at 3475 cm^{-1} may be assigned to the (OH)-stretching vibration of the (OH) group. The two weaker peaks at 3426 and 3288 cm^{-1}, and the peak at 1610 cm^{-1} are characteristic of the (NH)-stretching and H^{2+}–N^{3-}–H^{2+} bending vibrations, respectively, of the $(NH_2)^{-}$ group. Assuming the absorption coefficients of these two species to be similar, $(OH)^{-}$ seems to be the dominant group H-containing anion.

The utility of Fig. 6 is immediately apparent when considering the Raman spectrum of terlinguacreekite. The formula assigned to terlin-

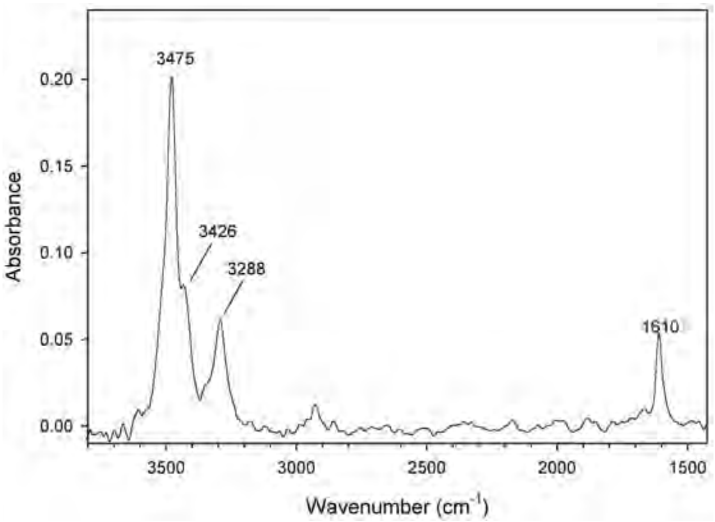

FIG. 7. The FTIR spectrum of comancheite.

TABLE 9. Comparison of the properties of comancheite from Roberts *et al.* (1981) and this work.

	Roberts *et al.* (1981)	This work
a (Å)	18.41(1)	18.414(5)
b	21.64(1)	21.328(6)
c	6.667(2)	6.698(2)
Symmetry	Orthorhombic	Orthorhombic
Space group	*Pnnm*/*Pnn*2	*Pnnm*
Density	Observed = 7.7(4)	Calculated = 8.3
Colour	Orange-red to yellow	Orange-red
Lustre	Vitreous	Vitreous
Habit	Massive to acicular	Massive to acicular
Mohs hardness	2	~2
Locality	Mariposa mine, Texas	Mariposa mine, Texas

	Chemical composition		
	EMPA	SREF	EMPA
Hg	83.1	84.45	86.3
Cl	5.1	6.65	6.1
Br	8.9	5.81	6.1
Total	97.1	96.91	98.5
N	–	2.57	–
O	–	0.49	–
H	–	0.03	–
Total	97.1	100.00	98.5
Powder pattern		see Figure 8	

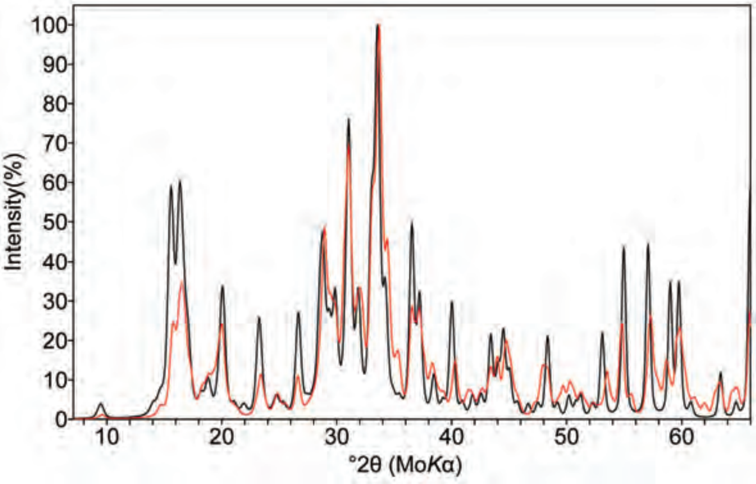

FIG. 8. Comparison of the reported X-ray powder-diffraction data for comancheite (Roberts *et al.*, 1981), black line, and comancheite single-crystal X-ray diffraction data (collapsed into two dimensions), red line. Traces were constructed using peak-shape criteria from the *Jade* software package using λ = 1.54178 Å.

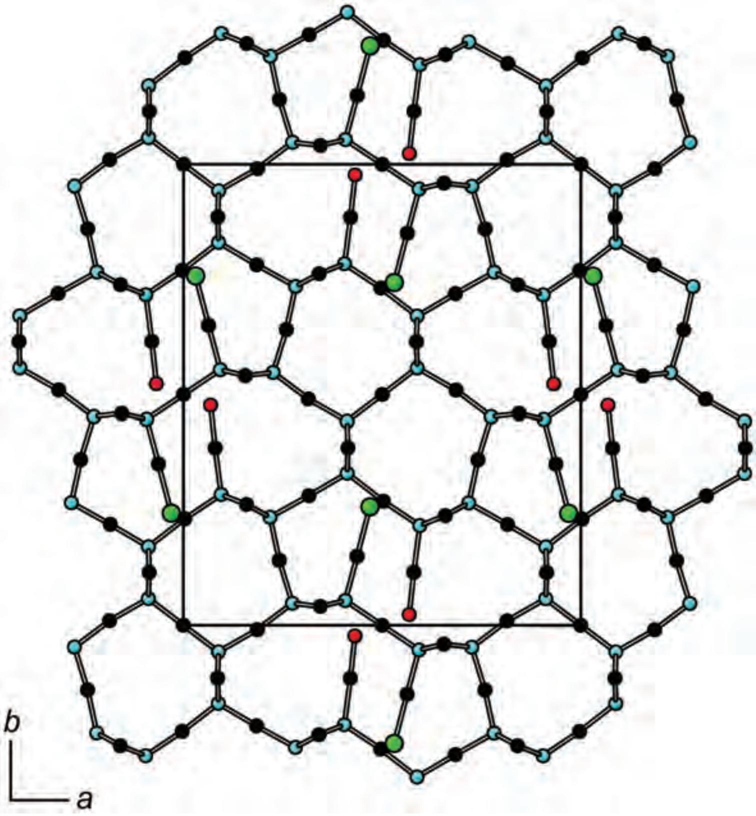

FIG. 9. The strong bonding of the $\{-\mathrm{Hg}^{2+}-\mathrm{N}^{3-}-\}$ net in comancheite viewed parallel to [001]; legend as in Fig. 1, black line: unit cell outline.

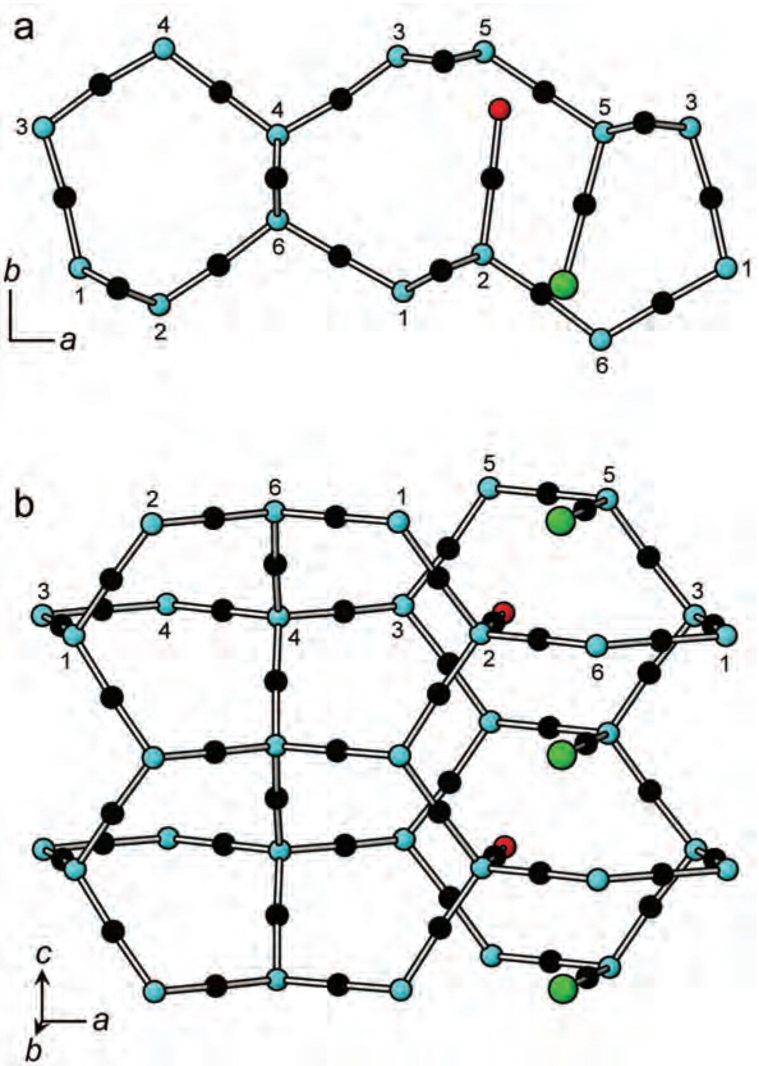

FIG. 10. The two unique $\{-Hg^{2+}-N^{3-}-\}$ rings in comancheite: (*a*) viewed parallel to [001]; (*b*) viewed from the side, down an axis rotated slightly from [010]; legend as in Fig. 1, numbers denote specific N^{3-} sites.

guacreekite (Roberts *et al.*, 2005) was $Hg_3O_2Cl_2$, and crystals were then not adequate for solution of the crystal structure. However, the Raman spectrum (Fig. 6) has its major peak at ~565 cm^{-1}, characteristic of a Hg nitride, and it is apparent that a revision of the chemical formula of terlinguacreekite is required.

The chemical formula of comancheite

The combined site-scattering results from structure refinement, electron-microprobe data and Raman and IR spectra suggest the following simplified formula ($Z = 1$) for comancheite:

$$Hg^{2+}_{55}N^{3-}_{24}(OH,NH_2)_4(Cl_{24.5}\ Br_{9.5})_{\Sigma=34}$$

When proposing a change to the formula for a mineral species, particularly a change as major as that involved for comancheite, it is necessary to ensure that one actually has a specimen of the mineral species in question. Table 9 compares the properties of comancheite from the Mariposa mine (Roberts *et al.*, 1981) with the analogous properties of comancheite (also from the

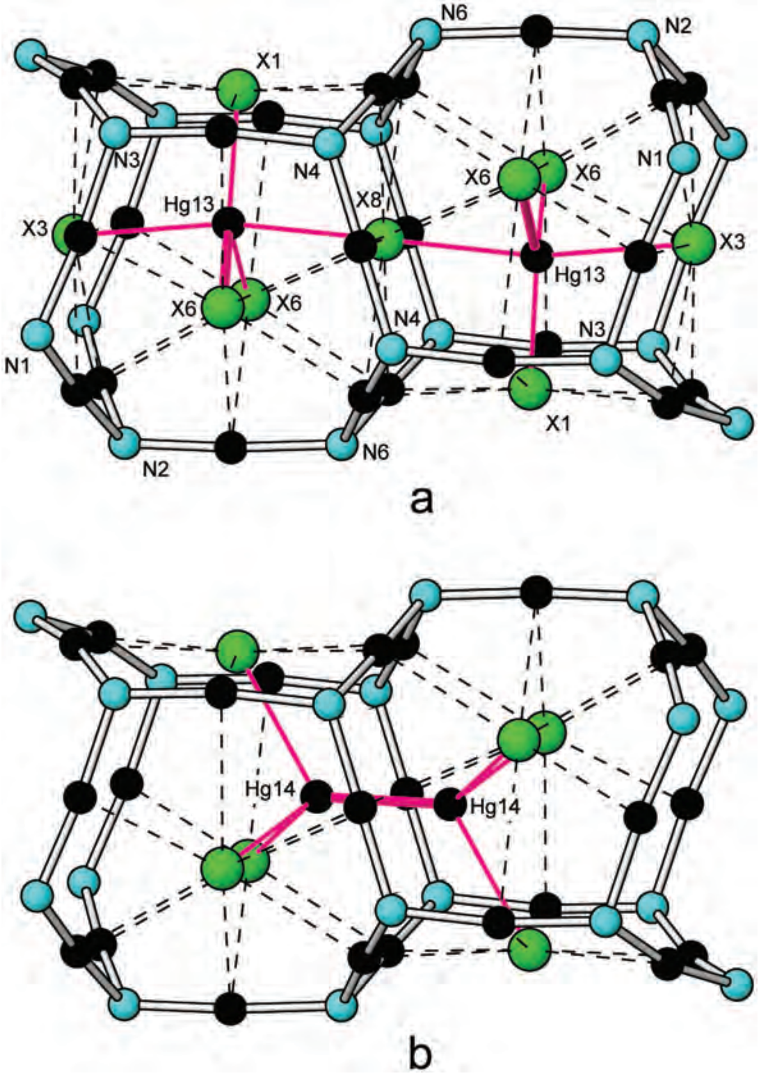

FIG. 11. A pair of neighbouring smaller $\{-Hg^{2+}-N^{3-}-\}$ rings in comancheite containing: (*a*) interstitial Hg^{2+} ions at *Hg*(13), or (*b*) interstitial $[Hg-Hg]^{2+}$ dimers at *Hg*(14), as viewed down an axis rotated slightly from [001]; legend as in Fig. 1, fuchsia lines: bonds between halide ions and interstitial Hg^{2+} ions; dashed lines: weaker bonds between halide ions and Hg^{2+} ions of the $\{-Hg^{2+}-N^{3-}-\}$ net.

Mariposa mine) from the Los Angeles County Museum, and Fig. 8 compares the experimental powder-diffraction pattern from Roberts *et al.* (1981) with the analogous pattern generated from the single-crystal X-ray data. The data for both samples show complete and close correspondence, indicating that we have examined comancheite in our structure work.

Structure connectivity

As mentioned previously, N^{3-} favours tetrahedral coordination by Hg^{2+}, and Hg^{2+} is typically coordinated by two N^{3-} anions in a near-linear $N^{3-}-Hg^{2+}-N^{3-}$ arrangement. This is the case for most of the comancheite structure as well, which leads to a strongly bonded three-dimensional

$\{-Hg^{2+}-N^{3-}-\}$ net within a sea of more weakly bound halide anions. As comancheite also contains a terminal $[(OH)^-,(NH_2)^-]$ group and a $N^{3-}-Hg^{2+}$-halide linkage, the three-dimensional net has two different interruptions to its main connectivity. A three-dimensional $\{-Hg^{2+}-N^{3-}-\}$ net can be relatively compact (e.g. kleinite, mosesite). On the other hand, a net can be expanded and possess internal cavities that are sufficiently large to contain additional interstitial Hg ions (e.g. comancheite contains interstitial Hg^{2+} and $[Hg-Hg]^{2+}$ dimers). The three-dimensional $\{-Hg^{2+}-N^{3-}-\}$ net of comancheite is shown in Fig. 9, looking down the short 6.7 Å *c* axis. There is a mirror plane perpendicular to [001] at z = ½ and the net extends along [001] into the page. The net terminations at the $[(OH)^-,(NH_2)^-]$ group and at the $N^{3-}-Hg^{2+}$-halide connection can be identified easily in Fig. 9. The net is characterized by two basic rings (when viewed along [001]) that are shown in Fig. 10*a*. When viewed (nearly) along [010], the connectivity between these basic rings along the *c* axis becomes apparent (Fig. 10*b*). The smaller ring with the N-atom sequence -1-3-4-4-6-2- (Fig. 10*a*) is adjacent to an identical ring across the origin (Fig. 9), and the interstitial Hg(13) and Hg(14) atoms are located within the interstices of this pair of rings (Fig. 11*a*,*b*). The larger ring with the N atom sequence -4-3-5-5-3-1-6-2-1-6- (Fig. 10*a*) is adjacent to an identical ring across the midpoint of a cell edge (Fig. 9), and the $[(OH)^-,(NH_2)^-]$ terminal anion-group sees an identical group across a central portal (-3-5-5-3-5-5-) (Fig. 12). The O(7)...O(7) separation through this portal is 2.70(5) Å, and may suggest a possible $O_D...O_A$ hydrogen-bond between neighbouring (OH) groups at O(7) through the portal. Where O(7) is occupied by $(NH_2)^-$, potential hydrogen-bond acceptor anions are less clear; there are X2 and X7 halogen atoms from 3.79 to 3.97 Å away from O(7).

Summary

Comancheite was originally described as an Hg-oxide mineral. However, solution of the crystal structure showed that the formulation of comancheite as an oxide is not compatible with

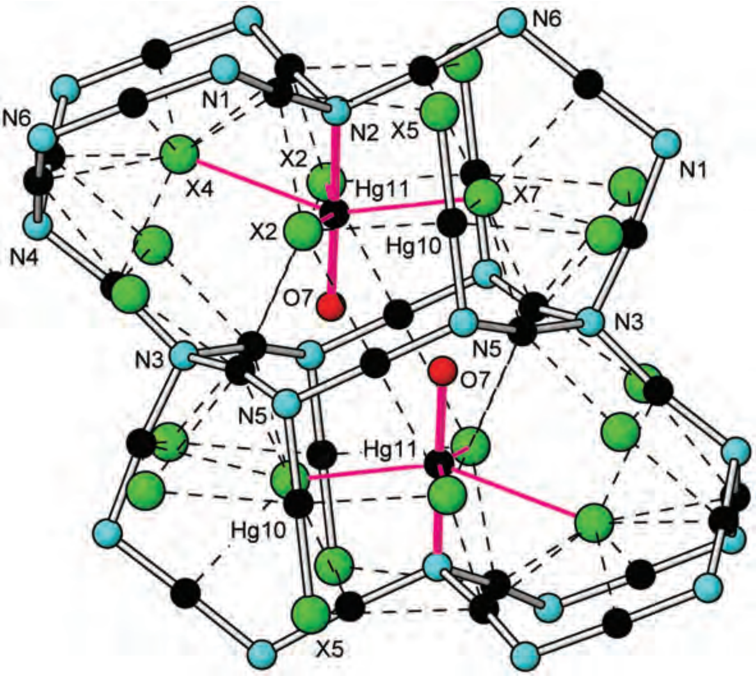

FIG. 12. A pair of neighbouring larger $\{-Hg^{2+}-N^{3-}-\}$ rings in comancheite that contain opposing terminal $(OH)^-$/$(NH_2)^-$ groups, as viewed down an axis rotated slightly from [001]. Legend as in Fig. 11.

electroneutrality, whereas formulation as a nitride gives a neutral formula. The bond-valence parameters for Hg^{2+}–N^{3-} were modified using accurately refined Hg-nitride structures, and give satisfactory incident bond-valence sums at the N^{3-} ions in these structures, allowing Hg^{2+}-nitride and Hg^{2+}-oxide structures to be distinguished. Examination of the Raman spectra of known Hg-nitride and Hg^{2+}-oxide structures shows that peaks in the range 500–700 cm^{-1} are characteristic of Hg^{2+}–N^{3-} stretching vibrations whereas peaks in the range 350–500 cm^{-1} are characteristic of Hg^{2+}–O^{2-} stretching vibrations; Hg^{2+}–O^{2-} and Hg^{2+}–N^{3-} bonds may be discriminated on this basis. Thus where there is insufficient material for chemical characterization of nitrogen *vs*. oxygen, and where microbeam methods are ineffective, bond-valence sums and Raman spectroscopy can distinguish Hg^{2+}-nitrides from Hg^{2+}-oxides. The Raman spectrum of terlinguacreekite indicates that it is a Hg^{2+}-nitride rather than a Hg^{2+}-oxide.

Acknowledgements

We thank Andy Roberts for suggesting that we look at the structure of comancheite, and three reviewers for their very helpful comments. This work was supported by a Canada Research Chair in Crystallography and Mineralogy and by Natural Sciences and Engineering Research Council of Canada Discovery, Equipment and Major Installation grants of the Natural Sciences and Engineering Research Council of Canada, and by Innovation grants from the Canada Foundation for Innovation to FCH.

References

Aurivillius, K. and Stålhandske, C. (1976) A neutron-diffraction study of trimercury(II)dihydroxide disulphate monohydrate, $Hg_3(OH)_2(SO_4)_2{\cdot}H_2O$. *Zeitschrift für Kristallographie*, **144**, 1–15.

Aurivillius, K. and Stålhandske, C. (1981) X-ray studies on the mercury(II) bromates $K_2Hg(BrO_3)_2(NO_3)_2$ and $Hg(BrO_3)_2{\cdot}2H_2O$. *Acta Chemica Scandinavica*, **35**, 537–544.

Björnlund, G. (1971) The crystal structure of $Hg(OH)BrO_3$. *Acta Chemica Scandinavica*, **25**, 1645–1654.

Borisov, S.V., Magarill, S.A., Pervukhina, N.V. and Peresypkina, E.V. (2005) Crystal chemistry of mercury oxo- and chalcohalides. *Crystallography Reviews*, **11**, 87–123.

Brese, N.E. and O'Keeffe, M. (1991) Bond-valence parameters for solids. *Acta Crystallographica*, **B47**, 192–197.

Bukvetskii, B.V., Polishchuk, S.A. and Simonov, V.I. (1976) Crystal structure of mercury difluoride dihydrate $HgF_2(H_2O)_2$. *Koordinatsionnaya Khimiya*, **2**, 1208–1212.

Cooper, M.A. and Hawthorne, F.C. (2003) The crystal structure of vasilyevite, $(Hg_2)^{2+}_{10}O_6I_3$ $(Br,Cl)_3(CO_3)$. *The Canadian Mineralogist*, **41**, 1173–1181.

Cooper, M.A. and Hawthorne, F.C. (2009) The crystal structure of tedhadleyite, $Hg^{2+}Hg^{1+}_{10}O_4I_2(Cl,Br)_2$, from the Clear Creek Claim, San Benito County, California. *Mineralogical Magazine*, **73**, 227–234.

Courant, E., Fourquet, J.L. and DePape, R. (1985) The crystal structure of $Hg_2FeF_5(OH)_2{\cdot}H_2O$. *Journal of Solid State Chemistry*, **60**, 343–346.

Fourquet, J.L., Courant, E., Chevalier, P. and De Pape, R. (1985) Structure of mercury(II) iron(III) fluoride dihydrate, $HgFeF_5.2H_2O$. *Acta Crystallographica*, **C41**, 165–167.

Giester, G., Mikenda, W. and Pertlik, F. (1996) Kleinite from Terlingua, Brewster County, Texas: investigations by single crystal X-ray diffraction, and vibrational spectroscopy. *Neues Jahrbuch für Mineralogie, Monatshefte*, **1996**, 49–56.

Göbbels, D. and Wickleder, M.S. (2004) Redetermination of mercury(II) hydroxide chlorate(V). *Acta Crystallographica*, **E60**, i40–i41.

Golovastikov, N.I. (1984) The crystal structure of mercury fluosilicate $Hg_2(OH)_2SiF_6(H_2O)_2$. *Soviet Physics Crystallography*, **29**, 359–360.

Hawthorne, F.C., Cooper, M. and Sen Gupta, P.K. (1994) The crystal structure of pinchite, $Hg_5Cl_2O_4$. *American Mineralogist*, **79**, 1199-1203.

Hawthorne, F.C, Ungaretti, L. and Oberti, R. (1995) Site populations in minerals: terminology and presentation of results of crystal-structure refinement. *The Canadian Mineralogist*, **33**, 907–911.

Johansson, G. and Sandström, M. (1978) The crystal structure of hexaaquamercury (II) perchlorate, $[Hg(H_2O)_6](ClO_4)_2$. *Acta Chemica Scandinavica*, **A32**, 109–113.

Koskenlinna, M. and Valkonen, J. (1996) Mercury(II) selenite hemihydrate. *Acta Crystallographica*, **C52**, 1070–1072.

Koskenlinna, M., Valkonen, J. and Fröhlich, R. (1996) Amminemercury(II) selenite. *Acta Crystallographica*, **C52**, 1072–1074.

Leineweber, A. and Jacobs, H. (2000) Kristallzucht und Strukturverfeinerung von Quecksilber(II)-amidchlorid – $HgClNH_2$. *Zeitschrift für anorganische und allgemeine Chemie*, 626, 2143–2145.

Martan, H. and Weiss, J. (1984) Metall-Schwefelstickstoff-Verbindungen. 17. Die Verbindungen $HgN_2S{\cdot}NH_3$ und $2Hg(NH_3)_2I_2{\cdot}S_4N_4$.

Zeitschrift für anorganische und allgemeine Chemie, **515**, 225–229.

Molla-Abbassi, A., Eriksson, L., Mink, J., Persson, I., Sandström, M., Skripkin, M., Ullström, A.-S. and Lindqvist-Reis, P. (2002) Structure and bonding of bisaquamercury(II) and trisaquathallium(III) trifluoromethanesulfonate *Journal of the Chemical Society, Dalton Transactions*, **2002**, 4357–4364.

Morzyk, B., Michalska, D., Wojciechowski W. and Glowiak T. (1999) Molecular structure of the novel 3-coordinated Hg(II) complex, aqua-bis(3,3-Dimethylglutarimidato)mercury (II). *Journal of Molecular Structure*, **478**, 99–105.

Nilsson, K.B., Maliarik, M., Persson, I., Fischer, A. Ullström, A.-S., Eriksson, L. and Sandström, M. (2008) Coordination chemistry of mercury(II) in liquid and aqueous ammonia solution and the crystal structure of tetraamminemercury(II) perchlorate. *Inorganic Chemistry*, **47**, 1953–1964.

Nockemann, P. and Meyer, G. (2002) Bildung von $NH_4[Hg_3(NH)_2](NO_3)_3$ und Umwandlung in $[Hg_2N](NO_3)$. *Zeitschrift für anorganische und allgemeine Chemie*, **628**, 2709–2714.

Nockemann, P. and Meyer, G. (2003) Zwei Mercuri-Ammin-Komplexe: $[Hg(NH_3)_2][HgCl_3]_2$ und $[Hg(NH_3)_4](ClO_4)_2$. *Zeitschrift für anorganische und allgemeine Chemie*, **629**, 123–128.

Nolte, M., Pantenburg, I. and Meyer, G. (2006) The monohydrate of basic mercuric nitrate, $[Hg(OH)](NO_3)(H_2O)$. *Zeitschrift für anorganische und allgemeine Chemie*, 632, 111–113.

Roberts, A.C., Ansell, H.G. and Dunn, P.J. (1981) Comancheite, a new mercury oxychloride-bromide from Terlingua, Texas. *The Canadian Mineralogist*, **19**, 393–396.

Roberts, A.C., Cooper, M.A., Hawthorne, F.C., Criddle, A.J., Stirling, J.A.R. and Dunning, G.E. (2002) Tedhadleylite, $Hg^{2+}Hg^{1+}_{10}O_4I_2(Cl,Br)_2$, a new mineral from the Clear Creek Claim, San Benito County, California. *The Canadian Mineralogist*, **40**, 909–914.

Roberts, A.C., Cooper, M.A., Hawthorne, F.C., Gault, R.A., Grice, J.D. and Nikischer, A.J. (2003*a*) Artsmithite, a new Hg^{1+}B-Al phosphate-hydroxide from the Funderburk Prospect, Pike County, Arkansas, U.S.A. *The Canadian Mineralogist*, **41**, 721–725.

Roberts, A.C., Cooper, M.A., Hawthorne, F.C., Stirling, J.A.R., Paar, W.H., Stanley, C.J., Dunning, G.E. and Burns, P.C. (2003*b*) Vasilyevite, $(Hg_2)^{2+}_{10}O_6I_3Br_2Cl(CO_3)$, a new mineral species from the Clear Creek Claim, San Benito, County, California. *The Canadian Mineralogist*, **41**, 1167–1172.

Roberts, A.C., Gault, R.A., Paar, W.H., Cooper, M.A., Hawthorne, F.C., Burns, P.C., Cisneros, S. and Foord, E.E. (2005) Terlinguacreekite, $Hg^{2+}_3O_2Cl_2$, a new mineral species from the Perry Pit, Mariposa Mine, Terlingua Mining District, Brewster County, Texas, U.S.A. *The Canadian Mineralogist*, **43**, 1055–1060.

Sandström M. (1978) An X-ray diffraction and Raman study of chloride, bromide, and iodide complexes of mercury(II) in dimethyl sulfoxide solution and of mercury(II) chloride in methanol solution. *Acta Chemica Scandinavia*, **A32**, 627–641.

Sheldrick, G.M. (2008) A short history of *SHELX*. *Acta Crystallographica*, **A64**, 112–122.

Stålhandske, C. (1978) A neutron diffraction study of mercury(II) selenate monohydrate. *Acta Crystallographica*, **B34**, 1408–1411.

Stålhandske, C. (1979) Refinement of mercury fluoride hydroxide. *Acta Crystallographica*, **B35**, 949–951.

Stålhandske, C. (1980) An X-ray and neutron diffraction study of mercury(II) sulphate monohydrate. *Acta Crystallographca*, **B36**, 23–26.

Stöger, B. and Weil, M. (2006) Hydrothermal crystal growth and crystal structures of the mercury(II) chromates(VI) α-$HgCrO_4$, β-$HgCrO_4$, and $HgCrO_4{\cdot}H_2O$. *Zeitschrift für Naturforschung B (Journal of Chemical Sciences)*, **61**, 708–714.

Weil, M. (2002*a*) Hydrothermal single crystal growth and crystal structures of the mercury(II) selenates(VI) $HgSeO_4$, $HgSeO_4{\cdot}HgO$ and $HgSeO_4{\cdot}2HgO$. *Zeitschrift für Naturforschung B (Journal of Chemical Sciences)*, **57b**, 1043–1050.

Weil, M. (2002*b*) The channel structure of the mercury(II) selenite(IV) oxide hydrate $HgSeO_3{\cdot}HgO{\cdot}{}^1/_6H_2O$. *Acta Crystallographica*, **C58**, i164–i166.

Weil, M. (2003) Single crystal growth, crystal structure and thermal behaviour of mercury(II) pyrophosphate dihydrate. *Monatshefte für Chemie*, **134**, 1509–1518.

Weil, M. (2005) Crystal structure of the mixed-valent basic mercury nitrate $Hg^I_2(NO_3)_2{\cdot}Hg^{II}(OH)(NO_3){\cdot}Hg^{II}(NO_3)_2{\cdot}4Hg^{II}O$ [= $Hg_8O_4(OH)(NO_3)_5$]. *Zeitschrift für anorganische und allgemeine Chemie*, **631**, 1346–1348.

Weil, M., Baumann, S. and Breitinger, D.K. (2008) $K_2[O(HgSO_3)_3]$, a new sulfitomercurate with an $[OHg_3]$ core. *Acta Crystallographica*, **C64**, i35–i37.